Supporting information

Photogenerated charges separation and recombination path modification in monocline Lu_2WO_6 via lattice transition and Bi-O antibonding states

Chunyu Zheng,[a‡] Ce Yu,[b‡] Han Yu,[a‡] Huibing Zheng,[c] Luqiao Yin,[d] Nian Fu,[e] Bangfu Ding,[b*] Liang Mao,[f*] Junying Zhang,[g]

[a]Key Laboratory of brain-like neuromorphic devices and systems of Hebei Province, College of Electron and Information Engineering, Hebei University, Baoding 071002, China; [b]College of Civil Engineering and Architecture, Hebei University, Baoding 071002, China;

[c]School of mathematics and physics, Anyang Institute of Technology, Anyang 455099, China

[d]Key Laboratory of Advanced Display and System Applications, Shanghai University, Ministry of Education, Shanghai 200444, China

[e]College of Physics Science and Technology, Hebei University, Baoding 071002, China;

[f]School of Materials Science and Engineering, China University of Mining and Technology, Xuzhou 221116, China

[g]School of Physics, Beihang University, Beijing 100191, China

Corresponding author. E-mail address: dbf1982@126.com and dingbangfu@gmail.com (B. F. Ding), E-mail: maoliang@cumt.edu.cn (L. Mao)

Table S1. Masses of raw materials in Bi-doped and $Bi^{3+}+RE^{3+}$-codoped samples

Samples (g)	WO_3	Lu_2O_3	Bi_2O_3	RE_2O_3
ω Bi	0.3478	(1-ω)×0.5969	ω×0.6989	0.0
1% Bi^{3+}+x Sm^{3+}	0.3478	(0.09-x)×0.5969	0.0070	x×0.5231
1% Bi^{3+}+y Eu^{3+}	0.3478	(0.09-y)×0.5969	0.0070	y×0.5279
1% Bi^{3+}+z Dy^{3+}	0.3478	(0.09-z)×0.5969	0.0070	z×0.5595
ω=0.005, 0.01, 0.03, 0.05, 0.10, 0.15, 0.20, 0.30, 0.40, 0.50				
x=0.01, 0.03, 0.05, 0.07, 0.10				
y=0.01, 0.05, 0.10, 0.15, 0.20				
z=0.005, 0.02, 0.04, 0.06, 0.08				

Table S2. All VCNEB parameters setting in INPUT file upon simulating monocline to perovskite phases transition

```
*****************************************
*        TYPE OF RUN AND SYSTEM        *
*****************************************
VCNEB      : calculationMethod

numSpecies
24   4    4    4
EndNumSpecies

atomType
O   Lu   W   Bi
EndAtomType

valences
2    3    6    3
endValences

0.00         : ExternalPressure
*****************************************
*            VCNEB options             *
*****************************************
111          : vcnebType
15           : numImages
143          : numSteps
1            : optimizerType
```

```
1              : optReadImages
3              : optRelaxType
0.1            : dt
0.005          : ConvThreshold


***********************
*        NEB options      *
***********************

0.3            : VarPathLength

3              : K_min

6              : K_max

0              : optFreezing

0              : optMethodCIDI
****************************************
*              OUTPUT                  *
****************************************

2              : FormatType

10             : PrintStep
****************************************
*   DETAILS OF AB INITIO CALCULATIONS *
****************************************

abinitioCode

1

ENDabinit


commandExecutable

yhrun -n 48 -p TH_NEW1 /vol6/home/user/bin/vasp >out

EndExecutable

1                : whichCluster

1                : numParallelCalcs
```

Table S3. Lobsterin file in COHP calculation for one, two, and three Bi^{3+}-doped monoclinic Lu_2WO_6

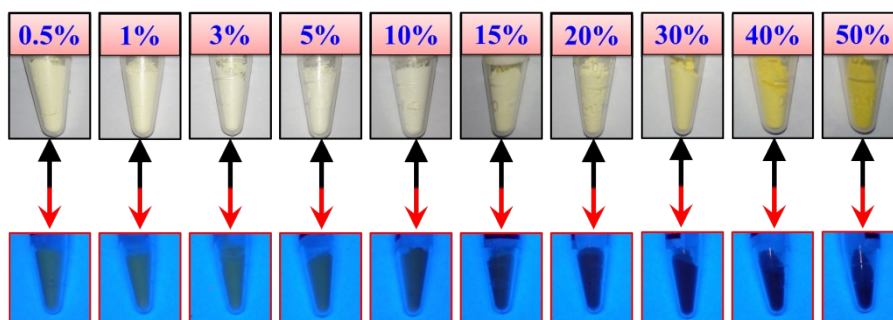| COHP Parameters	Values
COHPstartEnergy	-6
COHPendEnergy	10
basisSet	pbeVaspFit2015
basisfunctions	O 2s 2p W 5p 5d 6s Lu 4f 5s 5p 5d 6s Bi 5d 6s 6p
cohpGenerator	from p to q between atom I and atom II*
*p and q denoting bond length	

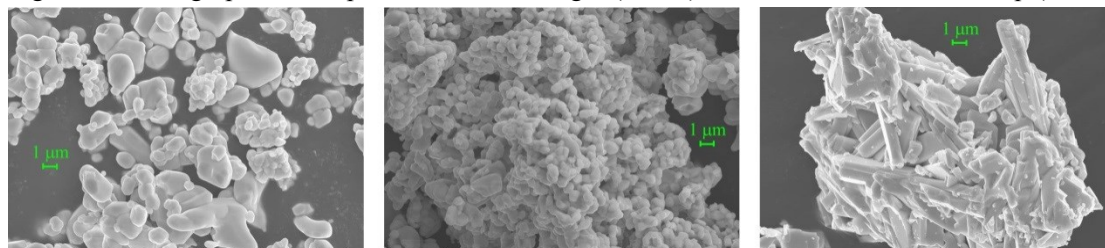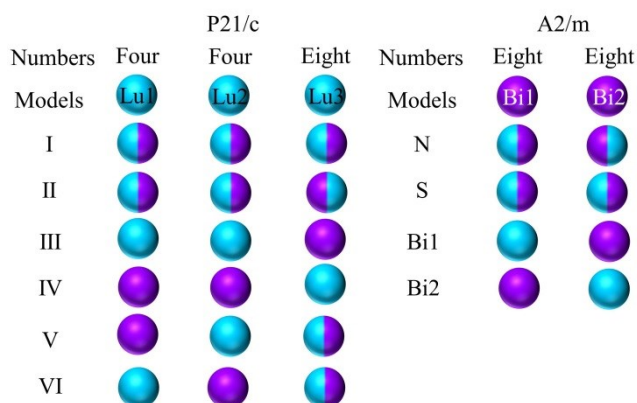Figure S1 Photographs of samples under natural light (above) and 365 nm ultraviolet damp (down)

Figure S2. High resolution SEM images of 1at% (a), 15at% (b), and 50at% (c) Bi-doped samples

Note: single and double colors denoting full and semi occupation.
semi replacement different Lu3 for models I and II
N and S representing neighbor and staggering occupation

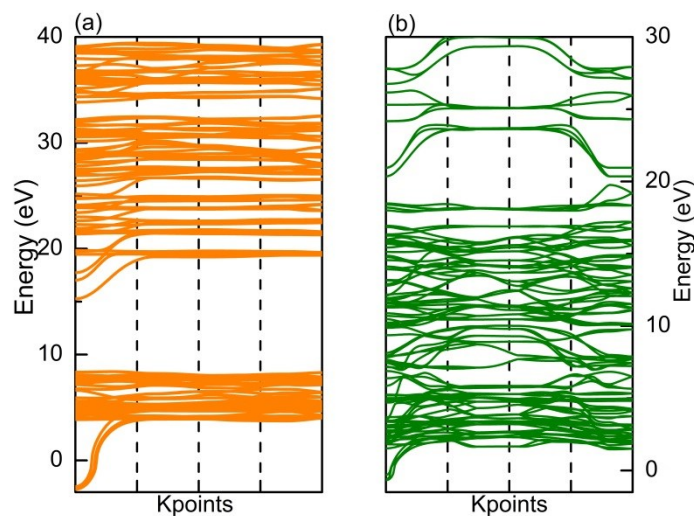Figure S3 Six P21/c and four A2/m 1×2×1 supercell models to obtain the lowest energy sites in initial and final images

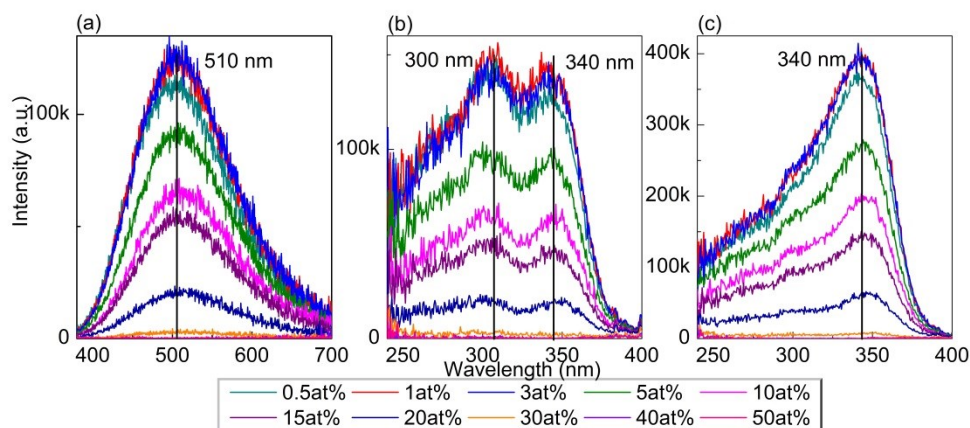Figure S4 phonon spectra with 2×2×1 P21/c (a) and 2×4×1 A2/m (b) supercell models calculations

Figure S5 Emission spectral with (a) λ_{ex}=300 nm as well as excitation spectrum with detection wavelengths (b) λ_{em}=450 nm and (c) λ_{em}=510 nm to Bi-doped samples
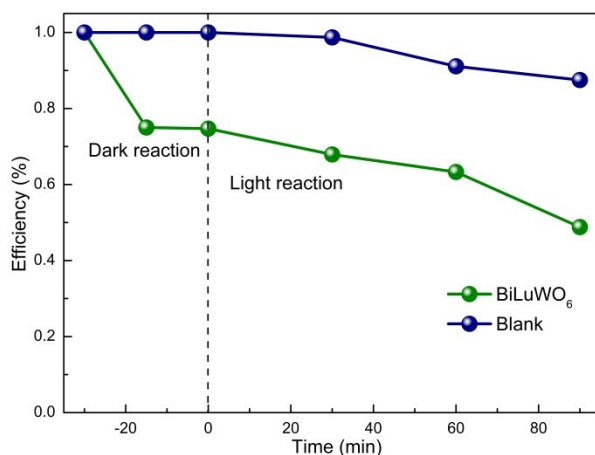

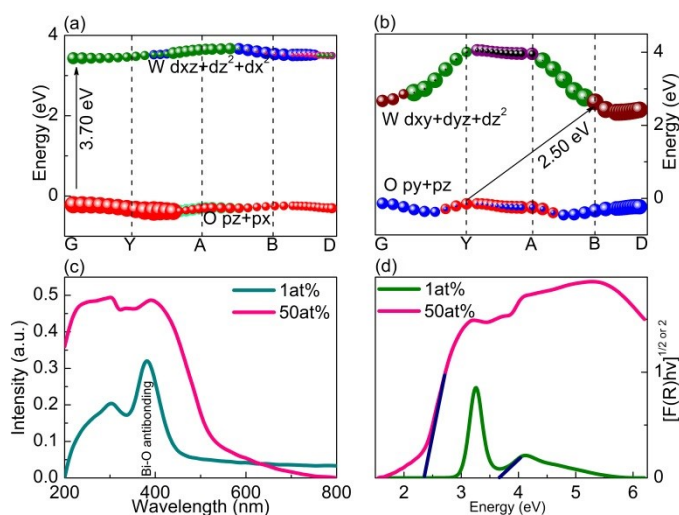Figure S6 Degradation efficiency of phenol under visible light condition

Figure S7 Energy band edge configuration of P21/c (a) and A12/m1 structures (b)Absorption spectrum (c) and Kubelka-Munk function fitting band gap values upon 1at% and 50at% Bi-doped samples (d)
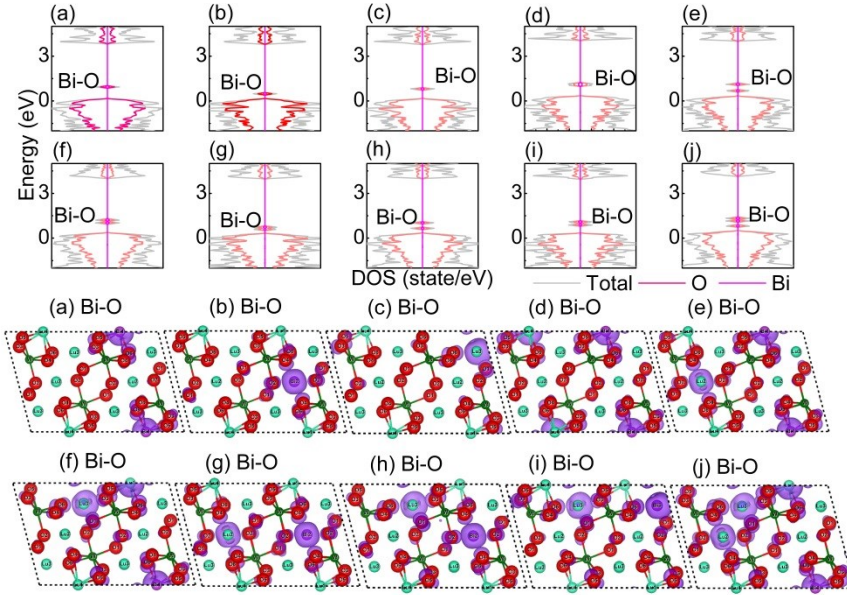
Figure S8 Total, projected DOS of $Lu1_{Bi}$ (a), $Lu2_{Bi}$ (b), $Lu3_{Bi}$ (c), $Lu1_{Bi}Lu1_{Bi}$ (d), $Lu1_{Bi}Lu2_{Bi}$ (e), $Lu1_{Bi}Lu3_{Bi}$ (f), $Lu2_{Bi}Lu2_{Bi}$ (g), $Lu2_{Bi}Lu3_{Bi}$ (h), $Lu3_{Bi}Lu3_{Bi}$ (i), $Lu1_{Bi}Lu2_{Bi}Lu3_{Bi}$ (j) models with Bi-O local state charge density in 0.007 e/Bohr^3 isosurface value

Figure S9 COHP of $Lu2_{Bi}Lu2_{Bi}$ (a) and $Lu1_{Bi}Lu2_{Bi}Lu3_{Bi}$ (b) models with Fermi levels 0 eV

Table S4. Bader charge of Bi^{3+} in three Lu sites for ten doping models

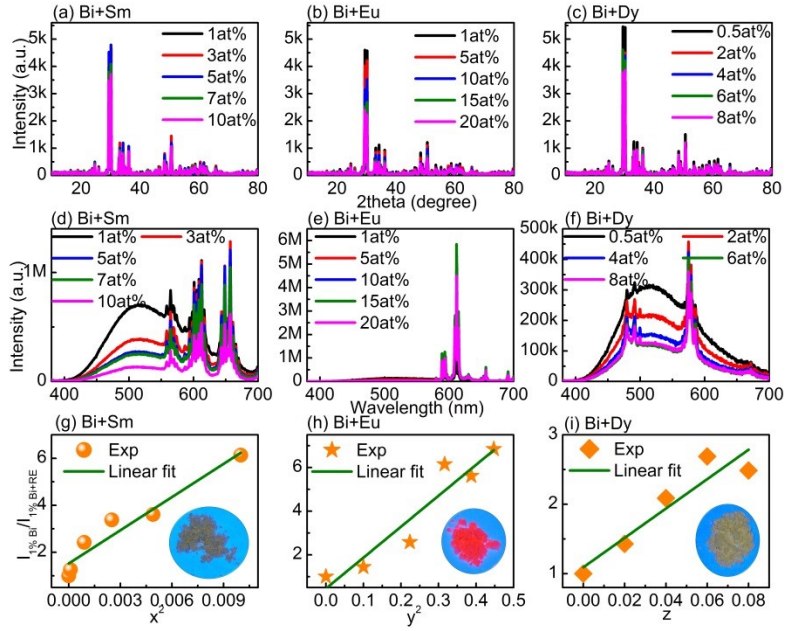| Models	Bi^{3+} charge numbers
$Lu1_{Bi}$	12.9635
$Lu2_{Bi}$	12.9093
$Lu3_{Bi}$	12.9436
$Lu1_{Bi}Lu1_{Bi}$	12.9658/12.9658
$Lu1_{Bi}Lu2_{Bi}$	12.9623/12.9138
$Lu1_{Bi}Lu3_{Bi}$	12.9610/12.9491
$Lu2_{Bi}Lu2_{Bi}$	12.9113/12.9113
$Lu2_{Bi}Lu3_{Bi}$	12.9118/12.9521
$Lu3_{Bi}Lu3_{Bi}$	12.9468/12.9468
$Lu1_{Bi}Lu2_{Bi}Lu3_{Bi}$	12.9611/12.9155/12.9378

Figure S10 XRD patterns (a), (b), (c), emission spectra of all codoped samples upon 340 nm excitation (d), (e), (f), and dependence relation of $I(Bi^{3+})/I(Bi^{3+}+RE^{3+})$ on x^2/y^2z^1 with photograph (g), (h), (i)

Table S5 Performance parameters of three LED damps

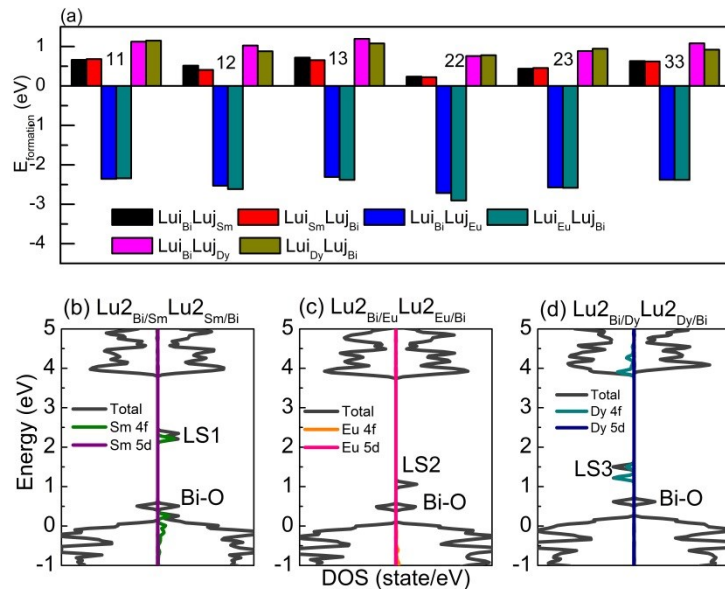| Samples	Current (mA)	Ra	Tc (K)	Purity (%)	Luminous Power (mW)
Bi+Sm	50	84.2	3914	53.3	1.024
	100	84.2	3963	52.1	2.067
	150	84.3	4005	51.4	3.051
Bi+Eu	50	49.5	1270	92.6	1.181
	100	59.6	1275	92.7	2.23
	150	50.4	1282	92.8	3.082
Bi+Dy	50	58.7	5001	47.3	0.6394
	100	58.4	5023	47	1.291
	150	59.6	5030	46.7	1.883

Figure S11 Formation energies of $Bi^{3+}+RE^{3+}$ models (a), density of states for the lowest formation

models (b), (c), and (d)

Table S6 Bader charge numbers of $Sm^{3+}/Eu^{3+}/Dy^{3+}$ in six typical models

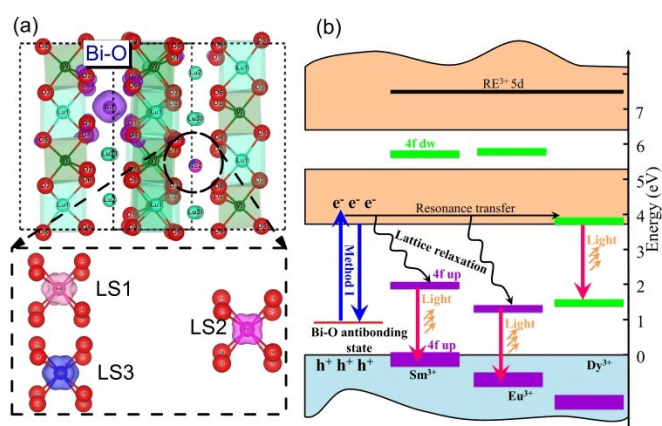| Models	RE^{3+} charge numbers
$Lu2_{Bi}Lu2_{Sm}$	13.9046
$Lu2_{Sm}Lu2_{Bi}$	13.9044
$Lu2_{Bi}Lu2_{Eu}$	14.8900
$Lu2_{Eu}Lu2_{Bi}$	14.8902
$Lu2_{Bi}Lu2_{Dy}$	17.8026
$Lu2_{Dy}Lu2_{Bi}$	17.8015

Figure S12 Bi-O antibonding state, LS1, LS2, and LS3 charge density with 0.007 e/Bohr^3 isosurface value (a) and recombination path modification using Bi-O antibonding and RE^{3+} 4f states (b)